Research Article

Xbp1s-Ddit3 promotes MCT-induced pulmonary hypertension

Hongxia Jiang[1,2], Dandan Ding[1,2], Yuanzhou He[1,2], Xiaochen Li[1,2], Yongjian Xu[1,2] and ⓘ Xiansheng Liu[1,2]

[1]Department of Pulmonary and Critical Care Medicine, Tongji Hospital, Tongji Medical College, Huazhong University of Science and Technology, Wuhan, China; [2]Key Laboratory of Pulmonary Diseases, National Ministry of Health of The People's Republic of China, Wuhan, China

Correspondence: Xiansheng Liu (doctorliu69@126.com)

Pulmonary hypertension (PH) is a life-threatening disease characterized by vascular remodeling. Exploring new therapy target is urgent. The purpose of the present study is to investigate whether and how spliced x-box binding protein 1 (xbp1s), a key component of endoplasmic reticulum stress (ERS), contributes to the pathogenesis of PH. Forty male SD rats were randomly assigned to four groups: Control, Monocrotaline (MCT), MCT+AAV-CTL (control), and MCT+AAV-xbp1s. The xbp1s protein levels were found to be elevated in lung tissues of the MCT group. Intratracheal injection of adeno-associated virus serotype 1 carrying xbp1s shRNA (AAV-xbp1s) to knock down the expression of xbp1s effectively ameliorated the MCT-induced elevation of right ventricular systolic pressure (RVSP), total pulmonary resistance (TPR), right ventricular hypertrophy and medial wall thickness of muscularized distal pulmonary arterioles. The abnormally increased positive staining rates of proliferating cell nuclear antigen (PCNA) and Ki67 and decreased positive staining rates of terminal deoxynucleotidyl transferase (TdT)-mediated dUTP nick end labeling (TUNEL) in pulmonary arterioles were also reversed in the MCT+AAV-xbp1s group. For mechanistic exploration, bioinformatics prediction of the protein network was performed on the STRING database, and further verification was performed by qRT-PCR, Western blots and co-immunoprecipitation (Co-IP). DNA damage-inducible transcript 3 (Ddit3) was identified as a downstream protein that interacted with xbp1s. Overexpression of Ddit3 restored the decreased proliferation, migration and cell viability caused by silencing of xbp1s. The protein level of Ddit3 was also highly consistent with xbp1s in the animal model. Taken together, our study demonstrated that xbp1s-Ddit3 may be a potential target to interfere with vascular remodeling in PH.

Introduction

Pulmonary hypertension (PH) is a disease defined by a mean pulmonary arterial pressure ≥25 mmHg within the low-pressure system of pulmonary circulation [1,2]. The combination of vasoconstriction, vascular remodeling and *in situ* thrombosis contributes to increased vascular resistance during the development of PH [3]. Recent therapies, including exogenous prostacyclin analogs, inhaled NO and sildenafil and endothelin receptor antagonists, are all based on the vasodilator hypothesis of PH [4]. The curative effects of these therapies are far from satisfactory, the prognosis of PH patients remains poor. Therapies targeting vascular remodeling urgently require further exploration. Medial wall thickening of distal pulmonary arterioles is the main abnormality contributing to the remodeling process, and the predominant cell component of the medial wall is pulmonary arterial smooth muscle cells (PASMCs) [5]. Therefore, elucidating the mechanisms that drive abnormal proliferation, migration, and apoptotic resistance of PASMCs during PH may provide clues to interfere with vascular abnormalities.

X-box binding protein (xbp1) is a member of the cyclic AMP response element binding protein/activating transcription factor family of transcription factors [6]. There are two isoforms of xbp1: unspliced xbp1 (xbp1u) and spliced xbp1 (xbp1s). Xbp1u is an inactive form, while xbp1s

is an active form that participates in endoplasmic reticulum stress (ERS). ERS occurs when cells are exposed to external or internal stress, such as hypoxia, perturbations in Ca^{2+} homeostasis, and protein folding defects. Cells initiate ERS to help cells restore homeostasis. It was reported previously that inhibitors of ERS, 4-phenylbutyric acid (4PBA) and hydrogen sulfide (H_2S) could mitigate the development of hypoxia and monocrotaline (MCT)-induced PH [7–11], but the underlying mechanism is still unclear.

Inositol-requiring enzyme 1 (IRE1), one of the three unfolded protein response (UPR) sensors, plays an important role in keeping ER homeostasis [6]. Upon ERS, IRE1α is activated, splicing 26 nucleotides from the open reading frame of the XBP1 mRNA and transforming it from xbp1u to xbp1s [12]. DNA damage-inducible transcript 3 (Ddit3) is a transcription factor during ERS that regulate a variety of genes involved in a broad range of physiological processes [13]. Although xbp1s and Ddit3 might be involved in the pathogenesis of PH in some studies, whether and how they influence the proliferation, migration, cell viability and apoptosis of PASMCs, and whether there is direct interaction between xbp1s and Ddit3 have not been demonstrated yet.

In the current study, we aimed to explore whether xbp1s plays a role in MCT-induced PH and tried to elucidate the underlying molecular interplay involved. Our *in vitro* and *in vivo* results demonstrated that xbp1s-Ddit3 could be the molecular axis that is responsible for the biological abnormalities of PASMCs, which eventually resulted in vascular remodeling and led to the development of PH.

Materials and methods
MCT-induced animal model of PH

The present study was approved by the Animal Experimentation Ethics Committee of Tongji Medical College, Huazhong University of Science and Technology, Wuhan, China. All animal care and experimental procedures conform to the guidelines from current NIH guidelines. Forty male Sprague-Dawley (SD) rats (weighing 140–190 g, aged 5 weeks) were obtained from Shulaibao Biotech (Wuhan) and housed in a specific pathogen-free (SPF) environment in Tongji Medical College Animal Center. Adeno-associated virus serotype 1 (AAV) was designed by Hanbio. The concentration was not below 10^{12} v.g/ml. Then, 150 μl of AAV1 carrying scrambled shRNA (AAV-CTL) or AAV-xbp1s was intratracheally injected into rats in the corresponding group. The dose of monocrotaline (MCT) was 60 mg/kg. Initially, MCT powder was dissolved in a solvent (ethanol:saline = 2:8), and rats were given an intraperitoneal injection of MCT to induce PH. Rats were randomly assigned to four groups: the control group, which was injected with MCT dissolvant; the MCT group, which was injected with MCT; and the MCT+AAV-CTL group, which was injected with MCT and AAV-CTL. The MCT+AAV-xbp1s group was injected with MCT and AAV-xbp1s. The time course of administration is described in Figure 1A. At killing, rats were anesthetized with sodium pentobarbital (60 mg/kg) through intraperitoneal infection and subjected to hemodynamic measurement. A well-designed catheter (Scicominc, U.S.A.) was placed in the right position through the right external jugular vein to measure right ventricular systolic pressure (RVSP, mmHg). A harder catheterization device (Scicominc, U.S.A.) was placed directly into the left carotid artery to measure systemic blood pressure (SBP, mmHg). Cardiac output measurements were obtained through a signal sensing and exaggeration system (mlt1402, ml313). Data were recorded using a PowerLab data acquisition system (ADInstruments, New Zealand).

HE staining, immunohistochemical staining and TUNEL assay

Lung tissues were fixed in 4% paraformaldehyde for 24 h, embedded in paraffin, sectioned at 4-μm thickness and stained with Hematoxylin and Eosin (H&E). For immunohistochemistry staining, paraffin-embedded lung sections were stained with α-SMA (GB111364, Servicebio, 1:1000), PCNA (GB11010, Servicebio, 1:500), and Ki67 (GB13030-2, Servicebio, 1:200). The terminal deoxynucleotidyl transferase (TdT)-mediated dUTP nick end labeling (TUNEL) assay was conducted with a Fluorescein (FITC) TUNEL Cell Apoptosis Detection Kit (Servicebio, G1501). It was designed to label the 3′-end of fragmented DNA of apoptotic cells, and green fluorescence represented positive staining. Procedures were performed according to the manufacturer's instructions.

Cell culture

Rats PASMCs were commercially obtained from iCELL (Shanghai) and passages 3–5 were applied for our experiments. Cells were grown in DME-F12 culture medium (HyClone) supplemented with 10% fetal bovine serum, 80 U/ml penicillin, and 0.08 mg/ml streptomycin. Normoxia (21% O_2, 5% CO_2, 37°C) or hypoxia (2% O_2, 5% CO_2, 37°C) was achieved in an airtight chamber (Thermo Fisher).
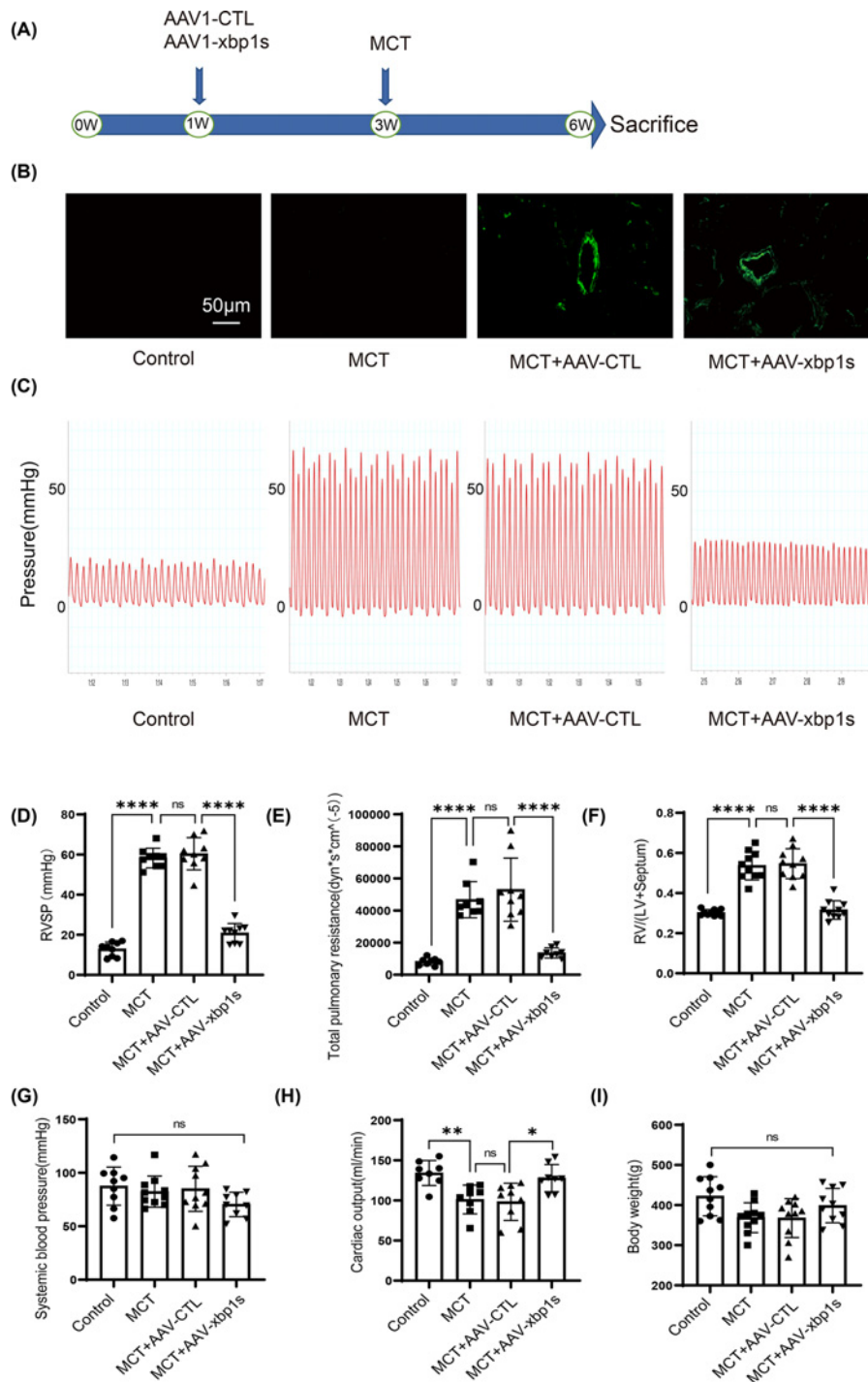
Figure 1. Knockdown of xbp1s mitigated MCT-induced PH

Forty SD male rats were randomly assigned to four groups. MCT was administered through intraperitoneal injection, and AAV was administered through intratracheal injection. AAV-xbp1s was designed to knock down the expression of xbp1s in rodents. Rats in the control group were injected with MCT dissolvant , the MCT group was injected with 60 mg/kg MCT, the MCT+AAV-CTL group was injected with MCT and AAV-carried scrambled shRNA (AAV-CTL), and the MCT+AAV-xbp1s group was injected with MCT and AAV-xbp1s. (**A**) Experimental design and time course of the rodent PH model. (**B**) Image captured by fluorescence microscopy to trace the location and expression of injected AAV in rodent lung tissues. (**C**) Representative image of RVSP measurement. Summarized data of RVSP (**D**), total pulmonary resistance (TPR) (**E**), right ventricular hypertrophy index (**F**), systemic blood pressure (SBP) (**G**), cardiac output (**H**) and body weight at killing (**I**). Data are represented as the mean $\pm$ SD, *n*=8–10. ns, no significance, *$P<0.05$, **$P<0.01$, ****$P<0.0001$.

qRT-PCR

Total RNA was extracted and purified from PASMCs, followed by reverse transcription to cDNA (TaKaRa RR036A) and cDNA amplification (TaKaRa, RR420A). Primer sequences are as follows: Xbp1s: forward: 5′-CTG AGT CCG CAG CAG GTG-3′, reverse: 5′-GAC CTC TGG GAG TTC CTC CA-3′. Ddit3: forward: 5′-GTC ACA AGC ACC TCC CAA AGC C-3′, reverse: 5′-CGC ACT GAC CAC TCT GTT TCC G-3′. Hsp90b1: forward: 5′-GGC CCT CAA GGA CAA GAT CG-3′, reverse: 5′-CTT GCC CGT CTG GTA TGC TT-3′. Hspa5: forward: 5′-GTG CCC ACC AAG AAG TCT CA-3′, reverse: 5′-AGG GGT CGT TCA CCT TCG TA-3′. Ern1: forward: 5′-GCG CAG GTG CAA TGA CAT AC-3′, reverse: 5′-CCT GCA GGA CTG GAT CTT CTT-3′. ATF2: forward: 5′-GTT CCT GTA CCA GGC CCA TT-3′, reverse: 5′-GAC TGG CCG AAC AAG TGG GA-3′. ATF3: forward: 5′-ATG TCA GTC ACC AAG TCT GAG G-3′, reverse: 5′-TCT CCA GTT TCT CTG ACT CCT TCT G-3′. ATF4: forward: 5′-CATG GGT TCT CCA GCG ACA A-3′, reverse: 5′-CCG GAA AAG GCA TCC TCC TTG-3′. ATF6: forward: 5′-ACG ACA GAG TCT CTC AGG TTG-3′, reverse: 5′-GCT GAG AAT TCG AGC CCT GT-3′. Creb1: forward: 5′-CAA ACA TAC CAG ATT CGC ACA G-3′, reverse: 5′-TCT CTT TCG TGC TGC TTC TT-3′. Actin: forward: 5′-CGT AAA GAC CTC TAT GCC AAC A-3′, reverse: 5′-CGG ACT CAT CGT ACT CCT GCT-3′. The relative quantifications were performed using the $2^{-\Delta(\Delta C_t)}$ method.

Western blot

Cells were harvested after the indicated treatments, and total protein was extracted using RIPA buffer (Servicebio). Proteins with different molecular weights were separated by SDS/polyacrylamide gel electrophoresis, and then, separated proteins on gels were transferred onto polyvinylidene fluoride (PVDF) membranes. The membranes were blocked in 5% skim milk for 1 h, rinsed with Tris-buffered saline with Tween 20 (TBST), incubated with diluted primary antibodies at 4°C for 24 h, rinsed again, and then incubated with secondary antibodies for 1 h at room temperature. After rinsing, the membrane was prepared for detection with SuperSignal West Femto Substrate (Thermo Fisher). Primary antibodies used are listed as follows: Xbp1s (CST, 40435s), Ddit3 (CST, 2895), Hsp90b1 (Proteintech,14700-1-AP), and Actin (Proteintech, 66009-1-Ig).

Co-immunoprecipitation

Cells were isolated in lysis buffer (Nonidet P-40: cocktail: PMSF: Phosphorylation protease inhibitor A: Phosphorylation protease inhibitor B = 1000:20:10:10:10:10). Xbp1s and rabbit IgG were immunoprecipitated from lysates with the corresponding primary antibodies: Xbp1s (CST, 40435s) and rabbit IgG (Beyotime, A7016). The immunoprecipitates were subjected to Western blots and incubated with Ddit3 primary antibody.

siRNA and plasmid transfection

Xbp1s-specific siRNA oligonucleotides were designed and purchased from RiboBio. The siRNA sequence of xbp1s was GATTGAGAACCAGGAGTTA (RiboBio). Plasmids designed to overexpress Ddit3 were purchased from Shanghai GeneChem. PASMCs were transiently transfected with siRNA or plasmid in Opti-MEM medium. In the experiments *in vitro*, when cells were transfected with siRNA to reduce the expression of xbp1s and transfected with plasmid to overexpress Ddit3. Scramble RNA and control vector of plasmid were transfected as the negative control, namely the 'NC' in the 'Hypoxia+NC' group. Transfection reagents were Lipo3000 and P3000 (Thermo). Assays were performed according to the manufacturer's recommendations.

EdU staining assay and cell viability assay

Cell proliferation was assessed by EdU incorporation into PASMCs using a proliferation detection kit (Cell-Light™ EdU Apollo567 In Vitro Kit (RiboBio)). Cell viability was measured by Cell Counting Kit-8 assays (MCE, HY-K0301). Detailed procedures were performed according to instructions from the kit.

Transwell assay

Cell migration was assessed using a Transwell cell culture chamber (8 μm pore size, Corning). Equal numbers of 1.0 × 10⁴ cells in each group were seeded in the upper chamber, and then, cells were cultured under normoxia or hypoxia for 24 h followed by fixation, staining, washing, and picture capture.

PORTLAND
PRESS

Statistical analysis

GraphPad Prism (version 8.0) was used for statistical analysis. Data are expressed as the mean $\pm$ standard deviation (SD). All experiments were conducted for at least three independent replications. For comparisons within multiple groups, one-way ANOVA was applied. $P<0.05$ was considered statistically significant.

Results

Knockdown of xbp1s led to hemodynamic improvement in MCT-induced PH

To explore the role of xbp1s and Ddit3 in a rodent model of PH, we randomly assigned male SD rats aged 5 weeks to four groups, and after 1 week of accommodation to adapt to the housing environment, the rats were subjected to intratracheal injection of AAV-carried scrambled shRNA (AAV-CTL) as a negative control or AAV-carried xbp1s shRNA (AAV-xbp1s) to knock down the expression of xbp1s. After 2 weeks, the virus was expressed in rats, and then, we conducted intraperitoneal injection of MCT (60 mg/kg) to induce a PH model. Three weeks after MCT injection, the rats were anesthetized and killed for hemodynamic measurement (Figure 1A). Since AAV was designed to express enhanced green fluorescence protein (eGFP) as a reporter gene, we were able to trace the location and expression of the injected virus and confirmed that it was indeed expressed in pulmonary vessels (Figure 1B). MCT successfully induced PH manifested as significant elevation of RVSP (Figure 1C,D), total pulmonary resistance (TPR) (Figure 1E), and right ventricular hypertrophy (Figure 1F) and a decrease in cardiac output (Figure 1H). Administration of AAV-xbp1s that knocked down xbp1s expression alleviated all these manifestations. No alleviation was observed in the rats administered AAV-CTL. No impact on systemic blood or body weight was observed following administration of AAV or MCT (Figure 1G,I). In short, knockdown of xbp1s could improve hemodynamic deterioration in an MCT-induced PH model, relieving elevated RVSP, TPR and right ventricular hypertrophy and recovering cardiac output without impacting systemic blood pressure or body weight.

Knockdown of xbp1s ameliorated vascular thickening and muscularization of pulmonary arterioles

To evaluate the distal pulmonary vascular abnormalities in the MCT-induced PH model, we conducted histological studies. Distal pulmonary arterioles with a diameter of 50–200 μm were analyzed. HE staining showed that MCT administration resulted in significant vascular remodeling with remarkable medial wall thickening, which is a key characteristic of PH. Knockdown of xbp1s by intratracheal injection of AAV-xbp1s strikingly attenuated medial wall thickening (Figure 2A,C). Immunohistochemical staining of α-smooth muscle actin (α-SMA, a marker for smooth muscle cells) revealed that in the PH model group, the expression of α-SMA (evaluated by average optical density, AOD = (integrated optical density, IOD)/area) was notably higher in thickening vessels, which indicated neomuscularization of the distal pulmonary arterioles. Administration of AAV-xbp1s obviously decreased the muscularization level (Figure 2B,D). We also detected the protein level of xbp1s in the lung tissues of rats in each group. Notably, the protein level of xbp1s increased nearly four-times in the MCT group compared with that in the control group, and administration of AAV-xbp1s successfully knocked down the expression of xbp1s. Moreover, the Ddit3 protein level was consistent with the protein level of xbp1s, namely, up-regulated in the MCT group and down-regulated in the MCT+AAV-xbp1s group (Figure 2E). In summary, MCT induced vascular remodeling and muscularization of distal arterioles, accompanied by elevated protein levels of xbp1s and Ddit3 in the lung tissues of rats. Administration of AAV-xbp1s decreased the protein level of xbp1s and attenuated vascular remodeling and muscularization.

Knockdown of xbp1s suppressed MCT-induced proliferation and apoptotic resistance of pulmonary arterioles

Vascular remodeling in PH is largely due to proliferation and apoptosis imbalance within the vascular wall [14]. To evaluate whether there is such an imbalance in the MCT-induced PH model, we performed immunohistochemical staining of PCNA and Ki67 to assess proliferation, and a TUNEL assay to assess apoptosis. PCNA and Ki67 are classic proliferative biomarkers, and positively stained cell rates were strongly increased in the MCT and MCT+AAV-CTL groups. Administration of AAV-xbp1s with knockdown of xbp1s largely decreased the positive staining rates (Figure 3A,C,D), indicating that knockdown of xbp1s suppressed the activated proliferation state of cell components within the vascular wall. TUNEL is a widely used method to detect apoptotic cells in tissue sections, and cells that undergo extensive DNA degradation during the late stages of apoptosis will be positively stained [15]. We analyzed all arterioles with a diameter of 50–200 μm in the rats with PH but observed nearly no apoptotic cells in the thickened vascular
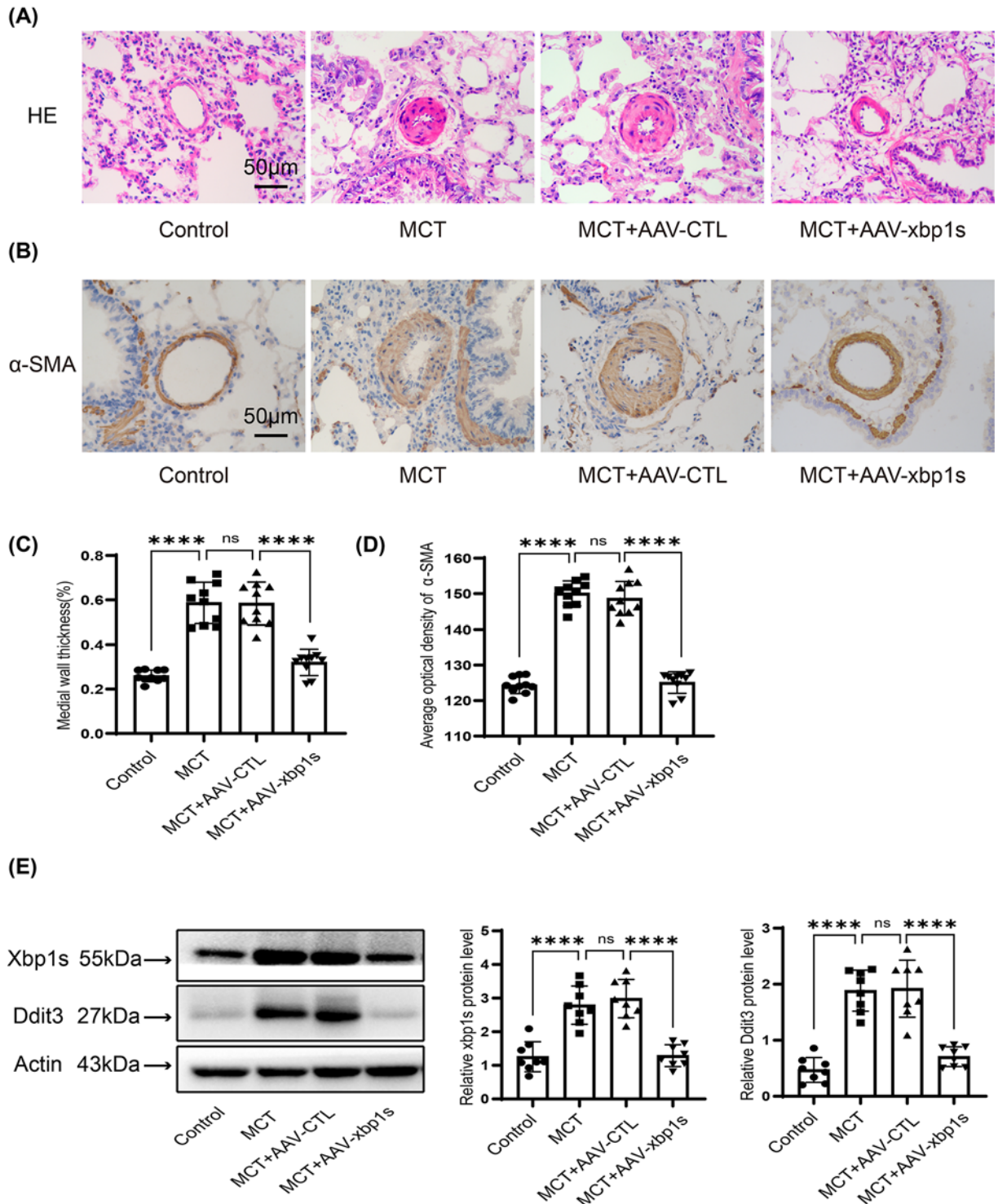
Figure 2. Knockdown of xbp1s alleviated MCT-induced vascular remodeling in the PH model
(**A**) Representative image of HE staining, which was performed to quantify the medial wall thickness of the distal pulmonary arterioles (original magnification, ×200). (**B**) Representative image of immunohistochemical staining of α-SMA, which reflects the muscularization of distal pulmonary arterioles (original magnification, ×200). Summarized data of HE staining (**C**) and average optical density of α-SMA (**D**). Medial wall thickness was calculated by the ratio of mean vessel thickness (μm) to mean outer vessel thickness (μm). (**E**) Representative Western blot and relative quantification analysis of xbp1s and Ddit3 protein expression in rodent PH model lung tissues. Data are represented as the mean $\pm$ SD, n=8–10. ns, no significance , ****$P < 0.0001$.
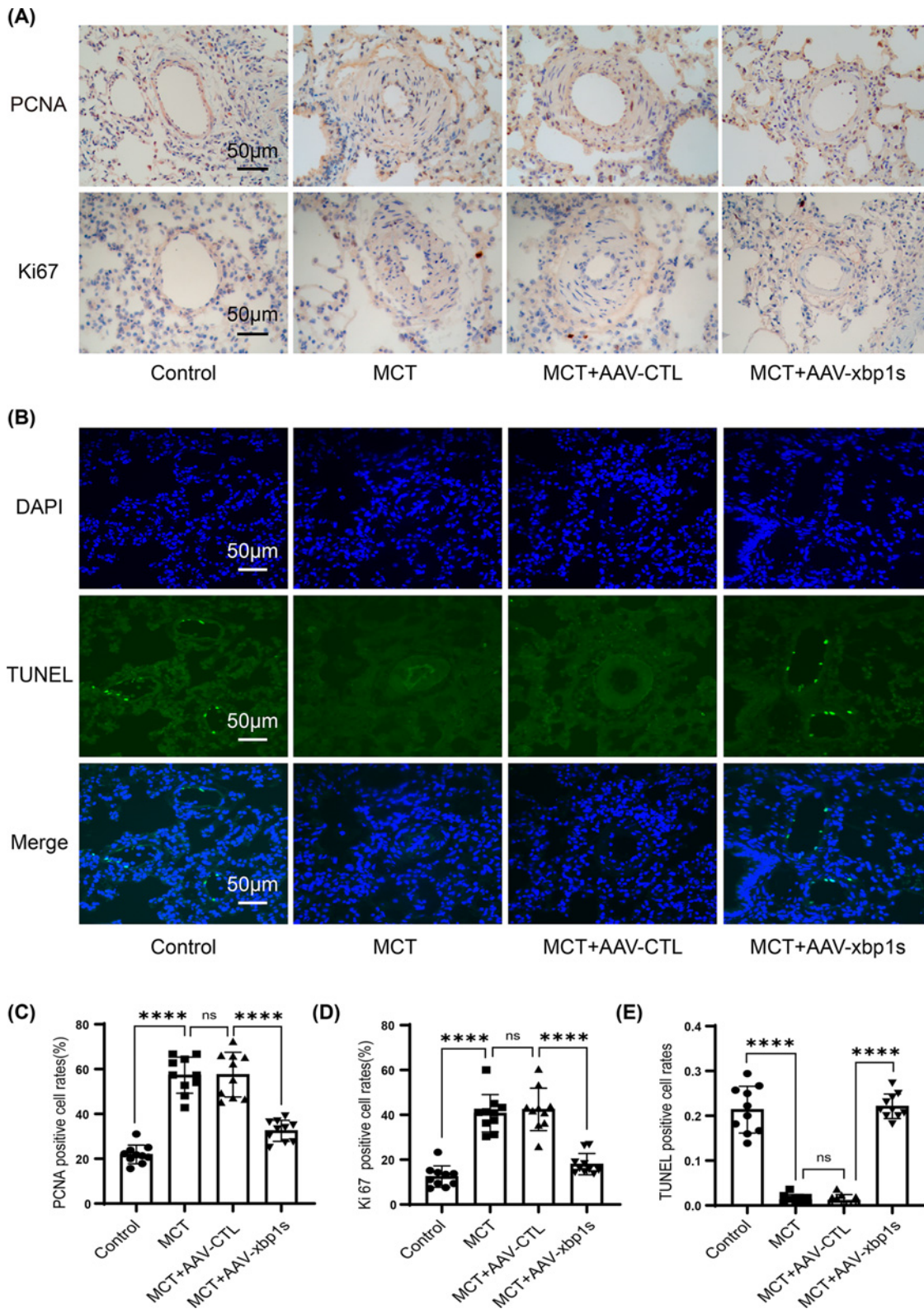
Figure 3. Knockdown of xbp1s restored MCT-induced proliferation and antiapoptotic effects in the PH model

(**A**) Representative image of immunohistochemical staining of PCNA and Ki67, which both reflect the proliferation of the detected sample. (**B**) Representative image of TUNEL staining. TUNEL-positive staining reflects the apoptotic state of the detected sample. Summarized data of PCNA- (**C**), Ki67- (**D**) and TUNEL- (**E**) positive rates. Data are represented as the mean $\pm$ SD, $n=10$. ns, no significance, ****$P<0.0001$.

wall; in other words, there was apoptotic resistance within the vascular wall, which would positively contribute to vascular remodeling. Correspondingly, in the rats injected with AAV-xbp1s, which developed less severe PH and a less thick vascular wall, the apoptotic rates returned to normal (Figure 3B,E). In short, in the MCT-induced PH model, there was an imbalance in proliferation and apoptosis within the vascular wall to promote arteriole thickening, and administration of AAV-xbp1s with knockdown of xbp1s returned it to a balanced state.

Bioinformatics analysis and verification of protein interactions with xbp1s

To identify the proteins that interact with xbp1s, we performed bioinformatics analysis with the STRING database, which is a comprehensive global resource providing protein–protein interaction analysis based on various clues [16,17]. First, we found that the protein ID of xbp1s (*Rattus norvegicus*) is Q9R1S4 on UniProt. Then, we used Q9R1S4 as a query protein on STRING. Under the term protein by sequence, we selected the organism as *R. norvegicus*. Then, we obtained the protein network shown in Figure 4A, and we identified ten associated proteins: ATF2, ATF4, ATF6, Hspa5, Ddit3, Ern1, ATF3, Creb1, Hsp90b1, and Ppp1r15a. The network image is composed of nodes and edges. Different colored edges represent different kinds of evidence that are based on predicting interactions. Among all the associations, only Ppp1r15a is connected with a single yellow edge connection predicted from text mining, which is relatively weak evidence. The other nine proteins all have at least two edges connected with xbp1s, indicating evidence from at least two perspectives. Therefore, we next performed qRT-PCR to determine whether these molecules have a similar variation pattern with xbp1s. Based on our previous study, hypoxia can trigger ERS and up-regulate the expression of xbp1s, so we cultured PASMCs in normoxia, hypoxia and hypoxia with xbp1s silencing. Then, we detected the expression of the nine proteins described above to determine whether they are also up-regulated by hypoxia and down-regulated when xbp1s is silenced under hypoxia.

As Figure 4B shows, Ddit3, Hsp90b1 and ATF6 shared a similar variation pattern with xbp1s. ATF6 is a transmembrane protein located on the endoplasmic reticulum membrane; together with PERK and upstream of xbp1s-IRE1, they are three branches of ERS [18], which is inconsistent with a role as a putative downstream factor of xbp1s. Ddit3 and Hsp90b1 are proteins involved in crucial physiological processes such as apoptosis, cell survival, cell cycle control, and hormone signaling [19,20]. DNA damage was thought to be related to the proliferative and apoptosis-resistant phenotype observed in PH vascular cells [21]. And the accumulation of HSP90 in the mitochondria was reported to be a feature of PH-PASMCs and a key regulator of mitochondrial homeostasis contributing to vascular remodeling in PH [22]. Therefore, we next performed Western blotting to verify the expression levels of Ddit3 and Hsp90b1. As shown by the results (Figure 4C–F), although silencing of xbp1s resulted in a decrease in the HSP90b1 protein level, its expression was not up-regulated by hypoxia. HSP90b1 belongs to the HSP90 family, which is responsible for myriad cellular processes. There are different isoforms of HSP90; some are constitutively expressed, while some are only induced under stress conditions [23,24]. According to our results, HSP90b1 may belong to the constitutively expressed type, so hypoxia failed to up-regulate its expression. The other tested protein, Ddit3, showed a variation pattern that was highly consistent with xbp1s. Therefore, we further performed a co-immunoprecipitation (Co-IP) experiment to explore the relationship between xbp1s and Ddit3, and xbp1s was able to pull down Ddit3 in both normoxic and hypoxic conditions (Figure 4G). In conclusion, based on STRING database prediction, qRT-PCR verification, Western blot validation, and Co-IP exploration, we targeted Ddit3 as the protein that interacts with xbp1s.

Decreased proliferation, migration, and cell viability by silencing of xbp1s was restored by overexpressing Ddit3

Since we found that Ddit3 could interact with xbp1s, we next investigated whether it meditated the biological effect of xbp1s. Silencing xbp1s by transfecting siRNA and overexpressing Ddit3 by transfecting plasmids resulted in decreased expression of xbp1s and enhanced expression of Ddit3 (Figure 5A). PASMCs were cultured in different contexts, and hypoxia-induced up-regulation of xbp1s and Ddit3 expression, accompanied by enhanced proliferation (Figure 5B,F), migration (Figure 5C,G), and cell viability (Figure 5E). Silencing xbp1s by transfecting siRNA led to decreased expression of xbp1s and Ddit3, accompanied by reduced proliferation, migration, and cell viability. Importantly, overexpression of Ddit3 restored the biological effects caused by silencing xbp1s. But overexpression of Ddit3 had no significant effect on the up-regulated apoptosis rate (Figure 5D,H). Taken together, our study demonstrated that the protein levels of xbp1s and Ddit3 were positively related to the proliferation, migration, and cell viability of PASMCs. Ddit3 is a downstream effector of xbp1s, and Ddit3 overexpression restored the decreased proliferation, migration, and cell viability resulting from xbp1s silencing.
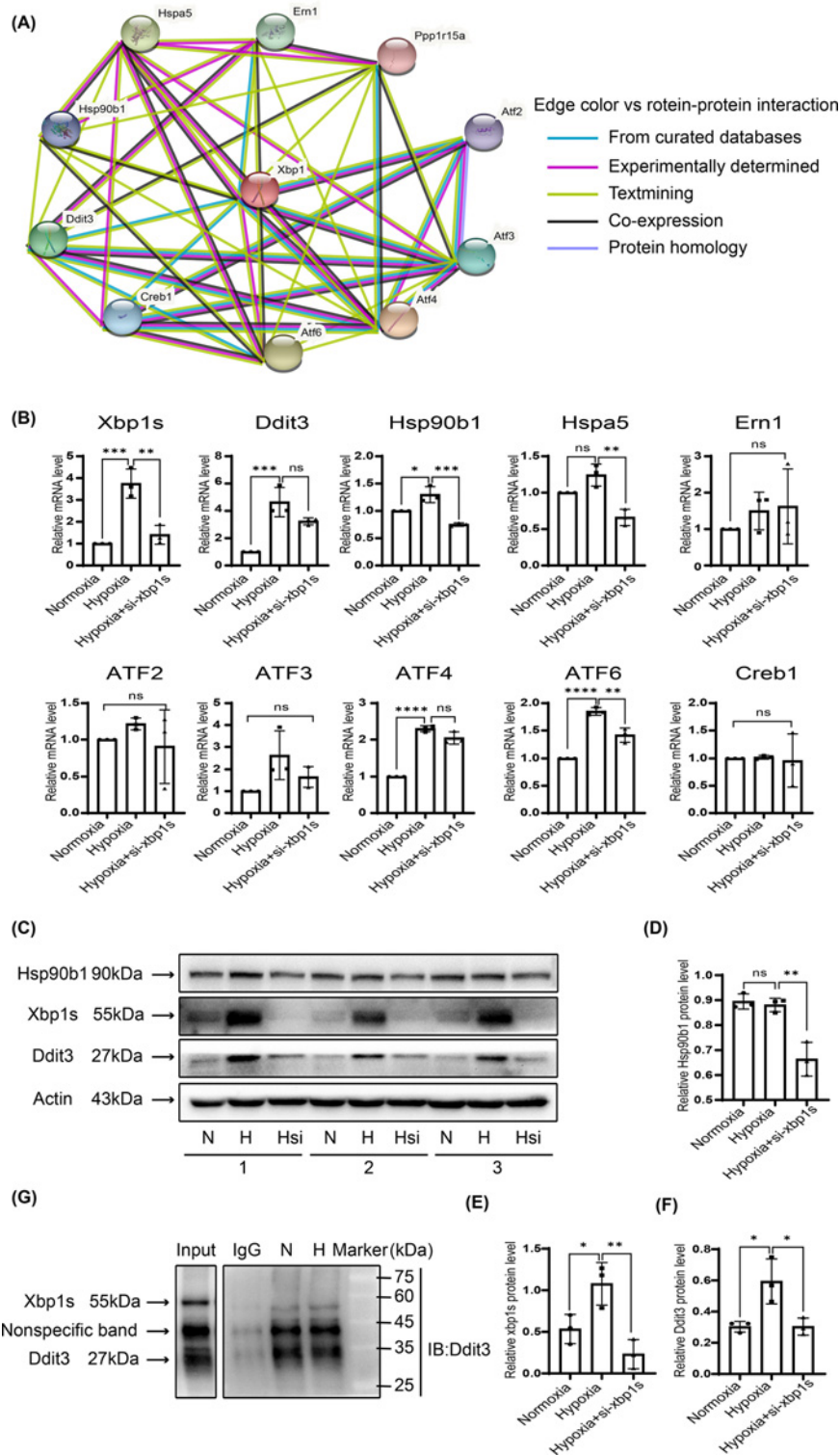
Figure 4. Proteins that interact with xbp1s

(**A**) Image showing the protein interaction network focused on xbp1s. Data were predicted by the STRING database. (**B**) qRT-PCR results showing the relative expression of proteins predicted to interact with xbp1s. Expression was detected in PASMCs cultured under normoxia, hypoxia, and hypoxia with xbp1s silencing. (**C**) Western blots showing xbp1s, Hsp90b1, and Ddit3 expression levels in PASMCs cultured in the indicated context. N-normoxia, H-hypoxia, Hsi-hypoxia+si-xbp1s. Relative quantification analysis of Hsp90b1 (**D**), xbp1s (**E**), and Ddit3 (**F**) shown in Figure 1(C). (**G**) Co-IP of Ddit3 with xbp1s. Data are represented as the mean $\pm$ SD, $n=3$. ns, no significance, *$P<0.05$, **$P<0.01$, ***$P<0.001$, ****$P<0.0001$. Abbreviation: Co-IP, co-immunoprecipitation.
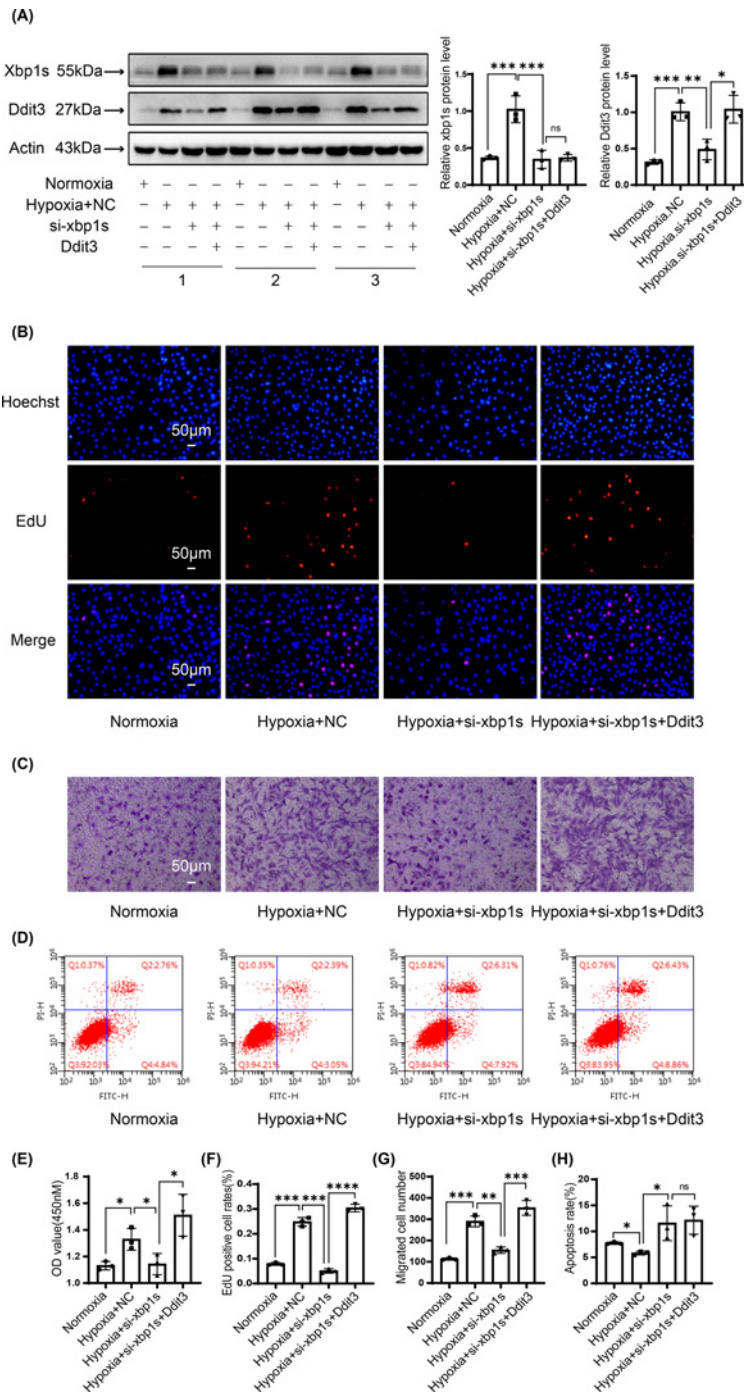
Figure 5. Overexpression of Ddit3 restored the proliferation rate, migration ability, and cell viability of rat PASMCs with silencing of xbp1s under hypoxia

(**A**) Western blots of xbp1s and Ddit3 and relative quantification analysis. PASMCs were cultured under normoxia, hypoxia with negative control transfection, hypoxia with siRNA transfection to silence xbp1s expression, hypoxia with cotransfection of siRNA to silence xbp1s and plasmid to overexpress Ddit3. (**B**) Representative image of the EdU staining assay, which was performed to detect the proliferation of PASMCs. (**C**) Representative image of the Transwell assay, which was performed to detect the migration ability of PASMCs. (original magnification, ×100). (**D**) Representative images and summary data of Annexin-V FITC/PI double staining. (**E**) Results of the cell viability assay, which was determined by Cell Counting Kit 8 (CCK-8). (**F**) Summarized data of EdU staining. (**G**) Summarized data of migrated cell numbers. (**H**) Summarized data of apoptosis rates. The early and late apoptosis rates were summed to calculate the total apoptosis rate. Data are represented as the mean $\pm$ SD, $n=3$. ns, no significance, *$P<0.05$, **$P<0.01$, ***$P<0.001$, ****$P<0.0001$.

Discussion

In the present study, we found that xbp1s was highly elevated in MCT-induced PH. Intratracheal injection of adeno-associated virus serotype 1 to knock down the expression of xbp1s (AAV-xbp1s) significantly attenuated MCT-induced increases in RVSP, TPR, right ventricular hypertrophy and the medial wall thickness of muscularized distal pulmonary arterioles. Abnormally increased proliferation and decreased apoptosis in arterioles were also reversed in the rats with MCT-induced PH after administration of AAV-xbp1s. To elucidate the underlying mechanisms mediating the function of xbp1s, we generated a protein–protein network (PPI) with the STRING database. Through verification using qRT-PCR, Western blots and Co-IP, we finally attested that Ddit3 could interact with xbp1s. Overexpression of Ddit3 restored the decreased proliferation, migration, and cell viability caused by silencing of xbp1s, and no significant effect on the increased apoptosis rate was observed. Taken together, our study demonstrates that the xbp1s-Ddit3 axis promotes MCT-induced PH, indicating this pathway could be a potential target for the treatment of PH.

As a potent transcription factor, xbp1s has been extensively studied in pulmonary diseases. In some case, xbp1s plays a protective role. In heart failure with preserved ejection fraction, the expression of xbp1s was found to be decreased in the myocardium of both rodent models and human patients, and overexpression of xbp1s in cardiomyocytes ameliorated the phenotype [25]. In heart ischemia/reperfusion, xbp1s acts as a protective factor in response to injury [26,27]. Xbp1s mediates cardioprotective effects in cardiac disease and heart failure [28]. Knockdown of xbp1s in endothelial cells decreased proliferation, knockout of xbp1s specifically in endothelial cells retarded early-stage retinal vasculogenesis and impaired angiogenesis in ischemic muscle tissues, and global deletion of xbp1s reduced vessel formation during embryonic development [29]. However, in some cases, xbp1s has a harmful effect. Xbp1s promoted the pathogenesis of idiopathic pulmonary fibrosis through regulation of muc5b [30]. Xbp1s expression was increased in mild asthma and associated with both type 2 inflammation and IFN-stimulated genes [31]. Xbp1s was found to play a positive role in promoting angiogenesis in both the tumor, cardiac, and brain vascular systems [29,32–36]. Regarding the role of xbp1s in PH, related research is very limited to our knowledge. However, there are some studies elucidating the role of ERS in PH. In both MCT- and hypoxia-induced PH animal models, administration of 4PBA, a well-known inhibitor of ERS, inhibited the three branches of ERS and concurrently attenuated PH manifested by decreasing pulmonary vascular resistance, pulmonary artery remodeling, and right ventricular hypertrophy [7–9,11]. Another inhibitor of ERS, H_2S, effectively inhibited hypoxia-induced increases in proliferation, migration, and oxidative stress in PASMCs. *In vivo* experiments further demonstrated that H_2S could prevent and reverse hypoxia-induced PH [10]. Xbp1s promoted the proliferation and migration of smooth muscle cells, leading to neointimal formation [37]. In this study, our experiments *in vivo* ascertained that xbp1s plays a harmful role in MCT-induced PH through induction of Ddit3. Administration of AAV1-xbp1s to knock down the expression of xbp1s reversed MCT-induced PH. Our experiments *in vitro* demonstrated that xbp1s positively affected the proliferation, migration, cell viability and apoptosis resistance in PASMCs. These results suggested that xbp1s and Ddit3 play an important role in regulating biological phenotypes of PASMCs and pathogenesis of MCT-PH.

The relationship between xbp1s and Ddit3 (C/EBP homologous protein, chop/CHOP) is under debate. In the context of the endoplasmic reticulum, chop is regulated by PERK-peIF2α-ATF4, and chop-GADD34-protein phosphatase 1 (PP1) dephosphorylates eukaryotic initiation factor-2 (eIF2α) in a negative feedback loop [38,39]. Among various studies, some have indicated that xbp1s negatively regulate the expression of chop. In cardiomyocytes, Sigma 1 receptor (Sigmar1)-dependent activation of IRE1-xbp1s was associated with inhibition of chop expression [40]. In chondrocytes and chondrosarcoma, si-xbp1s increased the expression and nuclear translocation of chop, while overexpression of xbp1s led to the opposite result [41]. In hepatocytes, *in vivo* and *in vitro* experiments demonstrated that knockdown of xbp1s increased the expression of chop [42]. Some studies have indicated that xbp1s is not associated with chop expression. In mouse embryo fibroblasts, chop was not significantly induced by xbp1s [43]. However, some studies also indicated that xbp1s positively regulated chop expression. Overexpression of xbp1s resulted in a nearly four-fold increase in chop mRNA levels, and chromatin immunoprecipitation (ChIP) assays demonstrated that xbp1s can bind to the promoter regions of chop genes [44]. In mesangial cells, xbp1s bound to the promoter region of chop and up-regulated chop expression [45]. The regulation of xbp1s and chop is controversial, and researchers obtained different conclusions in different cell lines and animal models. Here, in PASMCs, qRT-PCR and Western blots illustrated that the expression of chop was consistent with xbp1s, and silencing xbp1s led to a decrease in chop at both the mRNA and protein levels. Co-IP identified a direct interaction of xbp1s and chop. In short, our study revealed chop to be the downstream effector of xbp1s in PASMCs.

Ddit3, also referred to as growth arrest and DNA damage-inducible gene 153 (GADD153) or chop/CHOP, is a key component of ERS-induced apoptosis [13,46,47]. Ddit3 is a multifunctional transcription factor, and plays a dual role

both as an inhibitor of CCAAT/enhancer-binding protein (C/EBP) function and as an activator of other genes, which means it can both positively regulate a subset of genes and also negatively regulate another subset of genes [13,48]. When the endoplasmic reticulum can cope with stress, a series of responses are initiated to program the survival process. However, when facing severe and prolonged stress, the endoplasmic reticulum triggers a proapoptotic program via up-regulation of Ddit3 expression [20,46]. It was reported that inhibiting histone deacetylase 6 (HDAC6), which represents a new promising target to improve PH [49], was able to induce DNA damage, up-regulate the expression of Ddit3, and enhance cell death [50]. In rat cell lines, overexpression of chop resulted in down-regulation of bcl2 expression, depletion of cellular glutathione, and exaggerated production of reactive oxygen species, thus predisposing cells to ERS-induced apoptosis [51]. In mice, mouse embryonic fibroblasts (MEFs) derived from chop$^{-/-}$ animals exhibited apoptotic resistance compared with that of wildtype animals [52]. Although chop is widely known to function as a positive regulator of apoptosis, it also functions as a pro-proliferative factor in some cases. Overexpression of chop led to apoptosis in type-II alveolar epithelial cells but resulted in proliferation and collagen production in lung fibroblasts [53]. In research on atherosclerosis, chop was found to potentiate vascular smooth muscle cell (VSMC) proliferation and migration through the TRIB3/miR-208/TIMP3 axis [54]. In SM22α-CHOP-deficient mice, VSMC-specific CHOP deficiency displayed a reduced content of α-Actin-positive cells and decreased proliferation of aortic explant-derived VSMCs [55]. In our study, we confirmed that chop mediated the proliferative and migratory effects of xbp1s in PASMCs. Overexpression of chop restored the impaired proliferation and migration caused by silencing of xbp1s. However, overexpression of chop did not increase the apoptosis of PASMCs when xbp1s was silenced, probably because although overexpression of chop predisposes cells to ERS-induced apoptosis, it did not directly cause apoptosis when cells were not in a state of unresolved ERS. In the animal model, although the protein level of chop was obviously increased in hypertensive rats with significant vascular remodeling, TUNEL staining showed remarkably decreased apoptosis in thickened arterioles. We thought this was due to the imbalance between proliferation and apoptosis. On one hand, chop alone did not initiate apoptosis; on the other hand, a key component of thickened vessels, PASMCs, exhibited highly increased proliferation and migration rates when PH developed. Therefore, increased proliferation and migration played a predominant role and eventually resulted in the thickening of pulmonary arterioles. This finding is consistent with a study on high glucose-induced apoptosis in renal mesangial cells, in which the expression of chop was not positively related to apoptosis. In that case, chop participated in XBP1S-regulated necrosis but not apoptosis [45]. In brief, as a mediator of ERS apoptosis, overexpression of chop restored the proliferation and migration of PASMCs when xbp1s was silenced but did not increase the apoptotic rates.

There are some limitations of our study. Although MCT-induced PH is one of the most widely applied animal models to investigate PH, it does not display identical clinical manifestations as human PH [56]. MCT is activated to monocrotaline pyrrole (MCTP) by cytochrome P450 in the liver and then transported by red blood cells (RBCs) to the lung, triggering endothelial injury and eventually leading to MCT syndrome [57,58]. MCT syndrome is a series of injuries, including PH, alveolar edema, alveolar septal cell hyperplasia, myocarditis, hepatic veno-occlusive disease, and renal insufficiency [56,59]. Although PH is the main characteristic of MCT syndrome, injuries involving other organs are not associated with human PH.

To conclude, our study demonstrated that xbp1s and Ddit3 were highly elevated in the lung tissues of rodents with MCT-induced PH. Administration of AAV-xbp1s to knock down the expression of xbp1s alleviated MCT-induced increases in RVSP, TPR, right ventricular hypertrophy, and the medial wall thickness of muscularized distal pulmonary arterioles. Knocking down xbp1s was also able to mitigate the imbalance between proliferation and apoptosis in arterioles. The expression of Ddit3 was highly consistent with xbp1s, and Co-IP revealed a direct interaction of xbp1s and Ddit3. Overexpression of Ddit3 restored impaired proliferation, migration, and cell viability of PASMCs caused by silencing of xbp1s. These data demonstrated that xbp1s-Ddit3 could be a potential target for the treatment of PH.

Clinical perspectives

- PH is a disease with high morbidity and mortality, and elucidating the specific mechanism contributing to pathogenic development is urgently needed. Inhibitors of ERS were reported to mitigate PH. The present study was designed to determine whether and how xbp1s, a key factor of ERS, plays a role in the development of PH.

- Administration of AAV-xbp1s to knock down xbp1s was sufficient to ameliorate MCT-induced PH. Silencing xbp1s resulted in decreased proliferation, migration, and cell viability and increased apoptosis in PASMCs, while overexpression of Ddit3 reversed most effects.

PORTLAND
PRESS

- Recent therapies, including exogenous prostacyclin analogs, inhaled NO and sildenafil and endothelin receptor antagonists, are mainly focused on the vasodilator hypothesis of PH. Our study provides insights into interfering with vascular remodeling, the key process of PH pathogenesis, which could be a potentially important therapeutic strategy to prevent the irreversible vascular thickening process.

Data Availability

The data that support the findings of the present study are available from the corresponding author upon reasonable request.

Competing Interests

The authors declare that there are no competing interests associated with the manuscript.

CRediT Author Contribution

Hongxia Jiang: Conceptualization, Data curation, Software, Formal analysis, Validation, Investigation, Visualization, Methodology, Writing—original draft, Writing—review & editing. **Dandan Ding:** Conceptualization, Software, Formal analysis. **Yuanzhou He:** Conceptualization, Software, Formal analysis. **Xiaochen Li:** Conceptualization, Software, Formal analysis. **Yongjian Xu:** Resources, Project administration. **Xiansheng Liu:** Resources, Supervision, Funding acquisition, Project administration, Writing—review & editing.

Abbreviations

AAV, adeno-associated virus; chop/CHOP, C/EBP homologous protein; Co-IP, co-immunoprecipitation; Ddit3, DNA damage-inducible transcript 3; eIF2α, eukaryotic initiation factor-2; ERS, endoplasmic reticulum stress; H_2S, hydrogen sulfide; IRE1, inositol-requiring enzyme 1; MCT, monocrotaline; PASMC, pulmonary arterial smooth muscle cell; PCNA, proliferating cell nuclear antigen; PH, pulmonary hypertension; RVSP, right ventricular systolic pressure; SD, Sprague-Dawley; TPR, total pulmonary resistance; TUNEL, terminal deoxynucleotidyl transferase (TdT)-mediated dUTP nick end labeling; xbp1s, X-box binding protein 1, spliced; xbp1u, X-box binding protein 1, unspliced; α-SMA, α-smooth muscle actin; 4PBA, 4-phenylbutyric acid.

References

1 Hoeper, M.M., Bogaard, H.J., Condliffe, R., Frantz, R., Khanna, D., Kurzyna, M. et al. (2013) Definitions and diagnosis of pulmonary hypertension. *J. Am. Coll. Cardiol.* **62**, D42–D50, https://doi.org/10.1016/j.jacc.2013.10.032

2 Huber, L.C., Bye, H., Brock, M. and Swiss Society of Pulmonary Hypertension (2015) The pathogenesis of pulmonary hypertension–an update. *Swiss Med. Wkly* **145**, w14202

3 Stenmark, K.R. and Mecham, R.P. (1997) Cellular and molecular mechanisms of pulmonary vascular remodeling. *Annu. Rev. Physiol.* **59**, 89–144, https://doi.org/10.1146/annurev.physiol.59.1.89

4 Michelakis, E.D., Wilkins, M.R. and Rabinovitch, M. (2008) Emerging concepts and translational priorities in pulmonary arterial hypertension. *Circulation* **118**, 1486–1495, https://doi.org/10.1161/CIRCULATIONAHA.106.673988

5 Stenmark, K.R., Frid, M.G., Graham, B.B. and Tuder, R.M. (2018) Dynamic and diverse changes in the functional properties of vascular smooth muscle cells in pulmonary hypertension. *Cardiovasc. Res.* **114**, 551–564, https://doi.org/10.1093/cvr/cvy004

6 Ong, H.K., Soo, B.P.C., Chu, K.L. and Chao, S.H. (2018) XBP-1, a cellular target for the development of novel anti-viral strategies. *Curr. Protein Pept. Sci.* **19**, 145–154

7 Dromparis, P., Paulin, R., Stenson, T.H., Haromy, A., Sutendra, G. and Michelakis, E.D. (2013) Attenuating endoplasmic reticulum stress as a novel therapeutic strategy in pulmonary hypertension. *Circulation* **127**, 115–125, https://doi.org/10.1161/CIRCULATIONAHA.112.133413

8 Koyama, M., Furuhashi, M., Ishimura, S., Mita, T., Fuseya, T., Okazaki, Y. et al. (2014) Reduction of endoplasmic reticulum stress by 4-phenylbutyric acid prevents the development of hypoxia-induced pulmonary arterial hypertension. *Am. J. Physiol. Heart Circ. Physiol.* **306**, H1314–H1323, https://doi.org/10.1152/ajpheart.00869.2013

9   Wang, J.J., Zuo, X.R., Xu, J., Zhou, J.Y., Kong, H., Zeng, X.N. et al. (2016) Evaluation and treatment of endoplasmic reticulum (ER) stress in right ventricular dysfunction during monocrotaline-induced rat pulmonary arterial hypertension. *Cardiovasc. Drugs Ther.* **30**, 587–598, https://doi.org/10.1007/s10557-016-6702-1

10 Wu, J., Pan, W., Wang, C., Dong, H., Xing, L., Hou, J. et al. (2019) H2S attenuates endoplasmic reticulum stress in hypoxia-induced pulmonary artery hypertension. *Biosci. Rep.* **39**, BSR20190304, https://doi.org/10.1042/BSR20190304

11 Wu, Y., Adi, D., Long, M., Wang, J., Liu, F., Gai, M.T. et al. (2016) 4-Phenylbutyric acid induces protection against pulmonary arterial hypertension in rats. *PLoS ONE* **11**, e0157538, https://doi.org/10.1371/journal.pone.0157538

12 Senft, D. and Ronai, Z.A. (2015) UPR, autophagy, and mitochondria crosstalk underlies the ER stress response. *Trends Biochem. Sci.* **40**, 141–148, https://doi.org/10.1016/j.tibs.2015.01.002

13 Oyadomari, S. and Mori, M. (2004) Roles of CHOP/GADD153 in endoplasmic reticulum stress. *Cell Death Differ.* **11**, 381–389, https://doi.org/10.1038/sj.cdd.4401373

14 Vaillancourt, M., Ruffenach, G., Meloche, J. and Bonnet, S. (2015) Adaptation and remodelling of the pulmonary circulation in pulmonary hypertension. *Can. J. Cardiol.* **31**, 407–415, https://doi.org/10.1016/j.cjca.2014.10.023

15 Kyrylkova, K., Kyryachenko, S., Leid, M. and Kioussi, C. (2012) Detection of apoptosis by TUNEL assay. *Methods Mol. Biol.* **887**, 41–47, https://doi.org/10.1007/978-1-61779-860-3˙5

16 von Mering, C., Huynen, M., Jaeggi, D., Schmidt, S., Bork, P. and Snel, B. (2003) STRING: a database of predicted functional associations between proteins. *Nucleic Acids Res.* **31**, 258–261, https://doi.org/10.1093/nar/gkg034

17 von Mering, C., Jensen, L.J., Snel, B., Hooper, S.D., Krupp, M., Foglierini, M. et al. (2005) STRING: known and predicted protein-protein associations, integrated and transferred across organisms. *Nucleic Acids Res.* **33**, D433–D437, https://doi.org/10.1093/nar/gki005

18 Hetz, C., Zhang, K. and Kaufman, R.J. (2020) Mechanisms, regulation and functions of the unfolded protein response. *Nat. Rev. Mol. Cell Biol.* **21**, 421–438, https://doi.org/10.1038/s41580-020-0250-z

19 Hoter, A., El-Sabban, M.E. and Naim, H.Y. (2018) The HSP90 family: structure, regulation, function, and implications in health and disease. *Int. J. Mol. Sci.* **19**, 2560, https://doi.org/10.3390/ijms19092560

20 Hu, H., Tian, M., Ding, C. and Yu, S. (2018) The C/EBP homologous protein (CHOP) transcription factor functions in endoplasmic reticulum stress-induced apoptosis and microbial infection. *Front. Immunol.* **9**, 3083, https://doi.org/10.3389/fimmu.2018.03083

21 Ranchoux, B., Meloche, J., Paulin, R., Boucherat, O., Provencher, S. and Bonnet, S. (2016) DNA damage and pulmonary hypertension. *Int. J. Mol. Sci.* **17**, 990, https://doi.org/10.3390/ijms17060990

22 Boucherat, O., Peterlini, T., Bourgeois, A., Nadeau, V., Breuils-Bonnet, S., Boilet-Molez, S. et al. (2018) Mitochondrial HSP90 accumulation promotes vascular remodeling in pulmonary arterial hypertension. *Am. J. Respir. Crit. Care Med.* **198**, 90–103, https://doi.org/10.1164/rccm.201708-1751OC

23 Biebl, M.M. and Buchner, J. (2019) Structure, function, and regulation of the Hsp90 machinery. *Cold Spring Harb. Perspect. Biol.* **11**, a034017, https://doi.org/10.1101/cshperspect.a034017

24 Langer, T., Rosmus, S. and Fasold, H. (2003) Intracellular localization of the 90 kDA heat shock protein (HSP90alpha) determined by expression of a EGFP-HSP90alpha-fusion protein in unstressed and heat stressed 3T3 cells. *Cell Biol. Int.* **27**, 47–52, https://doi.org/10.1016/S1065-6995(02)00256-1

25 Schiattarella, G.G., Altamirano, F., Tong, D., French, K.M., Villalobos, E., Kim, S.Y. et al. (2019) Nitrosative stress drives heart failure with preserved ejection fraction. *Nature* **568**, 351–356, https://doi.org/10.1038/s41586-019-1100-z

26 Bi, X., Zhang, G., Wang, X., Nguyen, C., May, H.I., Li, X. et al. (2018) Endoplasmic reticulum chaperone GRP78 protects heart from ischemia/reperfusion injury through Akt activation. *Circ. Res.* **122**, 1545–1554, https://doi.org/10.1161/CIRCRESAHA.117.312641

27 Wang, Z.V., Deng, Y., Gao, N., Pedrozo, Z., Li, D.L., Morales, C.R. et al. (2014) Spliced X-box binding protein 1 couples the unfolded protein response to hexosamine biosynthetic pathway. *Cell* **156**, 1179–1192, https://doi.org/10.1016/j.cell.2014.01.014

28 Binder, P., Wang, S., Radu, M., Zin, M., Collins, L., Khan, S. et al. (2019) Pak2 as a novel therapeutic target for cardioprotective endoplasmic reticulum stress response. *Circ. Res.* **124**, 696–711, https://doi.org/10.1161/CIRCRESAHA.118.312829

29 Zeng, L., Xiao, Q., Chen, M., Margariti, A., Martin, D., Ivetic, A. et al. (2013) Vascular endothelial cell growth-activated XBP1 splicing in endothelial cells is crucial for angiogenesis. *Circulation* **127**, 1712–1722, https://doi.org/10.1161/CIRCULATIONAHA.112.001337

30 Chen, G., Ribeiro, C.M.P., Sun, L., Okuda, K., Kato, T., Gilmore, R.C. et al. (2019) XBP1S regulates MUC5B in a promoter variant-dependent pathway in idiopathic pulmonary fibrosis airway epithelia. *Am. J. Respir. Crit. Care Med.* **200**, 220–234, https://doi.org/10.1164/rccm.201810-1972OC

31 Bhakta, N.R., Christenson, S.A., Nerella, S., Solberg, O.D., Nguyen, C.P., Choy, D.F. et al. (2018) IFN-stimulated gene expression, type 2 inflammation, and endoplasmic reticulum stress in asthma. *Am. J. Respir. Crit. Care Med.* **197**, 313–324, https://doi.org/10.1164/rccm.201706-1070OC

32 Chen, X., Iliopoulos, D., Zhang, Q., Tang, Q., Greenblatt, M.B., Hatziapostolou, M. et al. (2014) XBP1 promotes triple-negative breast cancer by controlling the HIF1alpha pathway. *Nature* **508**, 103–107, https://doi.org/10.1038/nature13119

33 Duan, Q., Ni, L., Wang, P., Chen, C., Yang, L., Ma, B. et al. (2016) Deregulation of XBP1 expression contributes to myocardial vascular endothelial growth factor-A expression and angiogenesis during cardiac hypertrophy in vivo. *Aging Cell* **15**, 625–633, https://doi.org/10.1111/acel.12460

34 Romero-Ramirez, L., Cao, H., Regalado, M.P., Kambham, N., Siemann, D., Kim, J.J. et al. (2009) X box-binding protein 1 regulates angiogenesis in human pancreatic adenocarcinomas. *Transl. Oncol.* **2**, 31–38, https://doi.org/10.1593/tlo.08211

35 Shi, S., Tang, M., Li, H., Ding, H., Lu, Y., Gao, L. et al. (2019) X-box binding protein I splicing attenuates brain microvascular endothelial cell damage induced by oxygen-glucose deprivation through the activation of phosphoinositide 3-kinase/protein kinase B, extracellular signal-regulated kinases, and hypoxia-inducible factor-1alpha/vascular endothelial growth factor signaling pathways. *J. Cell. Physiol.* **234**, 9316–9327, https://doi.org/10.1002/jcp.27614

36 Zhang, M., Tang, M., Wu, Q., Wang, Z., Chen, Z., Ding, H. et al. (2020) LncRNA DANCR attenuates brain microvascular endothelial cell damage induced by oxygen-glucose deprivation through regulating of miR-33a-5p/XBP1s. *Aging (Albany N.Y.)* **12**, 1778–1791, https://doi.org/10.18632/aging.102712

37 Zeng, L., Li, Y., Yang, J., Wang, G., Margariti, A., Xiao, Q. et al. (2015) XBP 1-deficiency abrogates neointimal lesion of injured vessels via cross talk with the PDGF signaling. *Arterioscler. Thromb. Vasc. Biol.* **35**, 2134–2144, https://doi.org/10.1161/ATVBAHA.115.305420

38 Malhi, H. and Kaufman, R.J. (2011) Endoplasmic reticulum stress in liver disease. *J. Hepatol.* **54**, 795–809, https://doi.org/10.1016/j.jhep.2010.11.005

39 Novoa, I., Zeng, H., Harding, H.P. and Ron, D. (2001) Feedback inhibition of the unfolded protein response by GADD34-mediated dephosphorylation of eIF2alpha. *J. Cell Biol.* **153**, 1011–1022, https://doi.org/10.1083/jcb.153.5.1011

40 Alam, S., Abdullah, C.S., Aishwarya, R., Orr, A.W., Traylor, J., Miriyala, S. et al. (2017) Sigmar1 regulates endoplasmic reticulum stress-induced C/EBP-homologous protein expression in cardiomyocytes. *Biosci. Rep.* **37**, https://doi.org/10.1042/BSR20170898

41 Guo, F.J., Liu, Y., Zhou, J., Luo, S., Zhao, W., Li, X. et al. (2012) XBP1S protects cells from ER stress-induced apoptosis through Erk1/2 signaling pathway involving CHOP. *Histochem. Cell Biol.* **138**, 447–460, https://doi.org/10.1007/s00418-012-0967-7

42 Liu, X., Henkel, A.S., LeCuyer, B.E., Schipma, M.J., Anderson, K.A. and Green, R.M. (2015) Hepatocyte X-box binding protein 1 deficiency increases liver injury in mice fed a high-fat/sugar diet. *Am. J. Physiol. Gastrointest. Liver Physiol.* **309**, G965–G974, https://doi.org/10.1152/ajpgi.00132.2015

43 Lee, A.H., Iwakoshi, N.N. and Glimcher, L.H. (2003) XBP-1 regulates a subset of endoplasmic reticulum resident chaperone genes in the unfolded protein response. *Mol. Cell. Biol.* **23**, 7448–7459, https://doi.org/10.1128/MCB.23.21.7448-7459.2003

44 Lew, Q.J., Chu, K.L., Lee, J., Koh, P.L., Rajasegaran, V., Teo, J.Y. et al. (2011) PCAF interacts with XBP-1S and mediates XBP-1S-dependent transcription. *Nucleic Acids Res.* **39**, 429–439, https://doi.org/10.1093/nar/gkq785

45 Shao, D., Ni, J., Shen, Y., Liu, J., Zhou, L., Xue, H. et al. (2015) CHOP mediates XBP1S-induced renal mesangial cell necrosis following high glucose treatment. *Eur. J. Pharmacol.* **758**, 89–96, https://doi.org/10.1016/j.ejphar.2015.03.069

46 Li, Y., Guo, Y., Tang, J., Jiang, J. and Chen, Z. (2014) New insights into the roles of CHOP-induced apoptosis in ER stress. *Acta Biochim. Biophys. Sin. (Shanghai)* **46**, 629–640, https://doi.org/10.1093/abbs/gmu048

47 Ron, D. and Habener, J.F. (1992) CHOP, a novel developmentally regulated nuclear protein that dimerizes with transcription factors C/EBP and LAP and functions as a dominant-negative inhibitor of gene transcription. *Genes Dev.* **6**, 439–453, https://doi.org/10.1101/gad.6.3.439

48 Chordata Protein Annotation Program DNA damage-inducible transcript 3 protein . https://www.uniprot.org/uniprot/Q62857

49 Boucherat, O., Chabot, S., Paulin, R., Trinh, I., Bourgeois, A., Potus, F. et al. (2017) HDAC6: a novel histone deacetylase implicated in pulmonary arterial hypertension. *Sci. Rep.* **7**, 4546, https://doi.org/10.1038/s41598-017-04874-4

50 Namdar, M., Perez, G., Ngo, L. and Marks, P.A. (2010) Selective inhibition of histone deacetylase 6 (HDAC6) induces DNA damage and sensitizes transformed cells to anticancer agents. *Proc. Natl. Acad. Sci. U.S.A.* **107**, 20003–20008, https://doi.org/10.1073/pnas.1013754107

51 McCullough, K.D., Martindale, J.L., Klotz, L.O., Aw, T.Y. and Holbrook, N.J. (2001) Gadd153 sensitizes cells to endoplasmic reticulum stress by down-regulating Bcl2 and perturbing the cellular redox state. *Mol. Cell. Biol.* **21**, 1249–1259, https://doi.org/10.1128/MCB.21.4.1249-1259.2001

52 Zinszner, H., Kuroda, M., Wang, X., Batchvarova, N., Lightfoot, R.T., Remotti, H. et al. (1998) CHOP is implicated in programmed cell death in response to impaired function of the endoplasmic reticulum. *Genes Dev.* **12**, 982–995, https://doi.org/10.1101/gad.12.7.982

53 Klymenko, O., Huehn, M., Wilhelm, J., Wasnick, R., Shalashova, I., Ruppert, C. et al. (2019) Regulation and role of the ER stress transcription factor CHOP in alveolar epithelial type-II cells. *J. Mol. Med. (Berl.)* **97**, 973–990, https://doi.org/10.1007/s00109-019-01787-9

54 Chen, R., Zhang, Y. and Zhao, C. (2021) CHOP increases TRIB3-dependent miR-208 expression to potentiate vascular smooth muscle cell proliferation and migration by downregulating TIMP3 in atherosclerosis. *Cardiovasc. Drugs Ther.*, https://doi.org/10.1007/s10557-021-07154-6

55 Zhou, A.X., Wang, X., Lin, C.S., Han, J., Yong, J., Nadolski, M.J. et al. (2015) C/EBP-homologous protein (CHOP) in vascular smooth muscle cells regulates their proliferation in aortic explants and atherosclerotic lesions. *Circ. Res.* **116**, 1736–1743, https://doi.org/10.1161/CIRCRESAHA.116.305602

56 Gomez-Arroyo, J.G., Farkas, L., Alhussaini, A.A., Farkas, D., Kraskauskas, D., Voelkel, N.F. et al. (2012) The monocrotaline model of pulmonary hypertension in perspective. *Am. J. Physiol. Lung Cell. Mol. Physiol.* **302**, L363–L369, https://doi.org/10.1152/ajplung.00212.2011

57 Roth, R.A. and Reindel, J.F. (1991) Lung vascular injury from monocrotaline pyrrole, a putative hepatic metabolite. *Adv. Exp. Med. Biol.* **283**, 477–487, https://doi.org/10.1007/978-1-4684-5877-0´64

58 Wilson, D.W., Segall, H.J., Pan, L.C., Lame, M.W., Estep, J.E. and Morin, D. (1992) Mechanisms and pathology of monocrotaline pulmonary toxicity. *Crit. Rev. Toxicol.* **22**, 307–325, https://doi.org/10.3109/10408449209146311

59 Carman, B.L., Predescu, D.N., Machado, R. and Predescu, S.A. (2019) Plexiform arteriopathy in rodent models of pulmonary arterial hypertension. *Am. J. Pathol.* **189**, 1133–1144, https://doi.org/10.1016/j.ajpath.2019.02.005